Identifying Asymptomatic Nodes in SIS Network Epidemics using Betweenness Centrality over Time

Conrado Catarcione Pinto[1], **Vitor Martins Gouvêa**[2], **Daniel Ratton Figueiredo**[1]

[1]Programa de Engenharia de Sistemas e Computação (PESC)
Universidade Federal do Rio de Janeiro (UFRJ)
Rio de Janeiro – RJ – Brazil

[2]Departamento de Matemática Aplicada
Universidade Federal do Rio de Janeiro (UFRJ)
Rio de Janeiro – RJ – Brazil

{conrado,daniel}@cos.ufrj.br, vitor.martins@matematica.ufrj.br

Abstract. *Identifying asymptomatic individuals (i.e., infected individuals who have no clear symptoms) during epidemic outbreaks is a critical challenge, as they can transmit the disease while remaining undetected. We address this problem using a network-based susceptible–infected–susceptible (SIS) probabilistic epidemic model, where only infected and symptomatic nodes are observable at any given time instant (i.e., an epidemic snapshot). We consider the observation of multiple snapshots, with a parameter that determines the inter-observation time interval. In order to identify the asymptomatic nodes, we introduce cumulative observed betweenness (COB), an extension of observed betweenness centrality that aggregates information across multiple snapshots. When evaluated against baseline methods across diverse network models and epidemic scenarios, COB consistently achieves higher precision, which improves monotonically with the number of snapshots. We further show that the interval between observations strongly affects performance, with widely spaced snapshots providing more informative data. These results demonstrate the potential of network-based inference for identifying asymptomatic individuals under limited testing resources.*

1. Introduction

Throughout history, societies have faced numerous epidemics and pandemics [Quammen 2012], often with catastrophic consequences. In many such outbreaks, including COVID-19 [Inui et al. 2020], a fraction of infected individuals do not exhibit clear symptoms while still transmitting the disease to others; these individuals are known as asymptomatic [Arons et al. 2020]. This "silent" transmission represents a serious challenge for public health, as the identification of infected individuals is crucial for controlling transmission rates and mitigating the overall impact of an epidemic. Although large-scale screening programmes could, in principle, detect asymptomatic individuals, such screening requires continuous and repeated testing of seemingly healthy populations, which is generally impractical and prohibitively expensive [López Seguí et al. 2021].

Despite the difficulty of testing entire populations, the identification of asymptomatic cases remains essential. This consideration motivates the development of accu-

rate and reliable alternative tools capable of complementing or even replacing widespread testing. Addressing this challenge is the main objective of this work.

Our approach is grounded in the framework of network science, whose well-established theoretical development and methodologies have demonstrated their suitability for modelling and analysing epidemic processes [Keeling and Eames 2005]. Within this context, we consider epidemics of the susceptible–infected–susceptible (SIS) type, in which individuals may become infected multiple times. Such recurrent infections are characteristic of diseases such as COVID-19 and influenza, for example. In this study, we assume that the asymptomatic or symptomatic nature of an individual is an intrinsic ("genetic") property. Consequently, regardless of the number of infections experienced, an individual either always exhibits symptoms when infected or never does.

Given the complexity of the SIS dynamics under consideration, we allow for multiple observations of the network epidemic over time. This sequence of observations provides additional information for the inference process and mitigates the loss of information arising from individuals who become infected, transmit the disease, and subsequently recover before observation. The observation process reveals nodes that are both symptomatic and infected at the instant the observation is made.

Our principal contribution lies in extending the **observed betweenness** centrality, originally introduced in [Pinto and Figueiredo 2024], to a more complex epidemiological setting. While that work considered the identification of asymptomatic individuals under a susceptible–infected (SI) network epidemic using a single observation, here we investigate its effectiveness within the more intricate SIS network epidemic using multiple observations. To this end, we evaluate the performance of the metric across a range of network models and epidemic scenarios. In particular, the time interval between successive observations is shown to be a fundamental parameter: observations that are close in time are much more correlated and thus provide less information about the asymptomatic nature of the nodes.

The method is benchmarked against alternative approaches, including a simple network centrality metric. Our results demonstrate that the precision of the observed betweenness method is consistently higher than that of the alternatives across all scenarios considered. These findings support its suitability as a reliable tool for the inference of asymptomatic individuals, even within the more challenging SIS network epidemic model.

The remainder of this paper is organised as follows. Section 2 reviews the relevant literature on the problem. Section 3 provides a detailed description of the epidemic model, including the treatment of asymptomatic individuals, the infection dynamics, and the random network models employed in this study. Section 4 introduces the methods proposed for inferring asymptomatic nodes. Section 5 presents the numerical evaluation setup and discusses the corresponding results. Finally, Section 6 offers concluding remarks and perspectives for future work.

2. Related Work

To our knowledge, few prior studies have addressed the identification of asymptomatic individuals during epidemic outbreaks. Their respective epidemic models and methodologies are summarised below.

[Chen et al. 2023] model asymptomatic as a transient state preceding infection confirmation and use TrustRank, with confirmed cases as seeds, to infer hidden infections. However, their evaluation is restricted to the top-ranked node, neglecting the overall quality of the ranking. [Zhang et al. 2023] consider a classical SIR model in which all infected nodes are initially unobserved and gradually revealed through daily screenings. They employ Bayesian inference to infer hidden infections from screening times, but their method relies on a locally tree-like network assumption that is rarely satisfied in practice. [Huang et al. 2023] consider infections that may be asymptomatic or confirmed, assuming the complete infection and recovery history of confirmed cases is known. They use Markov chain inference, updating infection probabilities using this detailed history, though this assumption of complete infection timelines is often unrealistic in real-world scenarios.

[Pinto and Figueiredo 2024] consider an SI model in which, after the epidemic is halted, only a fraction of infections is observed, while the remainder are treated as asymptomatic. They introduce a variant of the betweenness centrality measure, subsequently termed **observed betweenness**, which emphasises nodes that frequently lie on shortest paths between known infected nodes, thereby enabling the inference of hidden infections. This work raised the possibility of extending the method to SIS epidemics, although such an analysis fell outside its scope. The same metric was later incorporated by [Catarcione Pinto et al. 2026] as a node feature within a graph neural network evaluated under an analogous setting. In the present work, we adopt observed betweenness as our primary inference method.

Notably, we are not aware of any prior work addressing the identification of asymptomatic individuals in SIS epidemic settings, in which infected individuals can become susceptible again and thus cease to be observable, even if they were symptomatic during prior infectious periods.

3. Network Epidemic Model

Although epidemics have been studied through the lens of differential equations for over a century now [Bacaër 2011], more recent approaches rely on network models. By accommodating individual heterogeneity, network-based models are capable of capturing phenomena that more closely resemble real-world dynamics than approaches relying solely on aggregate descriptions via systems of differential equations.

Whether formulated through differential equations or network models, epidemic processes are modelled using a compartmental framework. In this setting, epidemiological states, such as susceptible (S), infected (I), recovered (R), and exposed (E), are predefined, and individuals transition between them while occupying only one compartment at any given time. This classical approach is adopted in the present work.

We consider a discrete-time susceptible–infected–susceptible (SIS) epidemic process unfolding over a fixed network (graph) $G = (V, E)$, where V and E denote the sets of nodes and edges, respectively. At each time step t, nodes are labelled according to their epidemiological state, forming a partition of V into susceptible, $S(t)$, and infected individuals, $I(t)$.

The epidemic process is initialised by selecting a subset of nodes uniformly at random from V and designating them as infected at time $t = 0$. The infection subsequently

propagates through the network via its edges according to the specified transmission dynamics. Specifically, each infected node $v \in I(t)$ independently attempts to infect each of its neighbours in $N(v)$ with probability $\beta > 0$ at every time step. Consequently, for a node $u \in S(t)$, the probability of becoming infected at time $t+1$ is given by

$$\mathbb{P}\left[u \in I(t+1) \mid u \in S(t)\right] = 1 - (1-\beta)^{r_u(t)},$$

where $r_u(t) = |N(u) \cap I(t)|$ denotes the number of infected neighbours of u at time t.

Recovery is also modelled as a random process. At each time step, an infected node $v \in I(t)$ recovers and becomes susceptible again with probability $\gamma > 0$, that is,

$$\mathbb{P}\left[v \in S(t+1) \mid v \in I(t)\right] = \gamma.$$

In addition to the epidemiological state, we assume that each node possesses an intrinsic and time-invariant characteristic determining whether it is symptomatic or asymptomatic when infected. Let $A \subseteq V$ denote the set of asymptomatic nodes. Then, symptomatic ($A^{\complement}$) and asymptomatic individuals form a partition of the node set. By construction, nodes in A never exhibit symptoms when infected, whereas nodes in $A^{\complement}$ are symptomatic whenever they are infected. Note that the epidemic process is oblivious to the asymptomatic or symptomatic nature of the node, as this property only affects the observations.

Finally, consider an observation (or snapshot) of the epidemic process at a given time t_s. Since only infected and symptomatic individuals can be identified, the set of observed infections is given by

$$O(t_s) = A^{\complement} \cap I(t_s). \tag{1}$$

This observation constitutes a key challenge: even if a node has been infected, has transmitted the disease to others, and is inherently symptomatic, its infection will remain unobserved if it has recovered before time t_s and is not infected again at time t_s.

3.1. Infection Analysis

We now analyse the infection dynamics in the neighbourhood of an infected node, regardless of whether it is symptomatic (and thus observable) or asymptomatic. To this end, we focus on the competition between two stochastic events: the recovery of the infected node and the transmission of the infection to its susceptible neighbours.

Due to the discrete-time structure of the model and the assumption that infection and recovery events occur independently according to Bernoulli trials, both processes follow geometric distributions. Let Y denote the time until recovery of an infected node $v \in I(t)$. Then, $Y \sim \mathrm{Geo}(\gamma)$. Similarly, for a susceptible neighbour $u \in N(v) \cap S(t)$, let X denote the time until u becomes infected by v. Then, $X \sim \mathrm{Geo}(\beta)$. This setting is illustrated in Figure 1. Importantly, in this analysis we ignore infections originating from nodes outside the immediate neighbourhood of v. Thus, the results should be interpreted as a local, first-order approximation of the spreading dynamics.

Let $d = |N(v) \cap S(t)|$ denote the number of susceptible neighbours of node v at time t, and let X_d be the random variable counting how many of these neighbours become

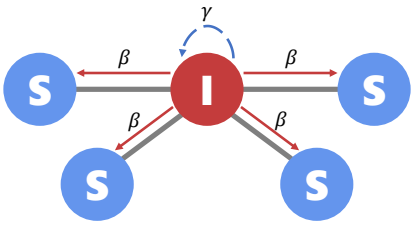

Figure 1. An infected node returns to the susceptible state with probability γ. During its infectious period, it attempts to infect each neighbour independently at every time step with probability β.

infected before v recovers. Conditioning on the recovery time $Y = t$, each neighbour is infected with probability $f_X(t) = \mathbb{P}[X \leq t] = 1 - (1-\beta)^t$. Hence,

$$\mathbb{E}[X_d \mid Y = t] = d\, f_X(t).$$

Taking the expectation over Y, we obtain

$$\begin{aligned}
\mathbb{E}[X_d] &= \sum_{t=1}^{\infty} \mathbb{E}[X_d \mid Y = t]\, \mathbb{P}[Y = t] \\
&= d\gamma \sum_{t=1}^{\infty} (1-\gamma)^{t-1} - d\gamma \sum_{t=1}^{\infty} (1-\beta)\left((1-\beta)(1-\gamma)\right)^{t-1} \\
&= d\frac{\beta}{\beta + \gamma - \beta\gamma}
\end{aligned}$$

Note that the expected number of neighbours that will be infected by v depends solely on β (transmission probability) and γ (recovery probability).

Finally, observe that when $\beta = \gamma \ll 1$, we have $\mathbb{E}[X_d] \approx \frac{d}{2}$. Hence, an infected node infects approximately half of its susceptible neighbours during its infectious period when both β and γ are small and equal.

3.2. Random Network Models

As stated previously, our model is formulated within a network-based framework. It is therefore appropriate to provide a brief overview of the network models employed in this study.

One of the most studied random graph models is the Erdős–Rényi model: given n nodes, each possible edge is independently included with probability p. Despite its tractability, it poorly represents real networks, whose degree distributions are typically heavy-tailed.

The Barabási–Albert model addresses this by generating growing networks [Albert and Barabási 2002]. Starting from a small graph, new vertices are added sequentially, each forming m links to existing nodes via preferential attachment, favouring high-degree nodes. This produces hubs and a power-law degree distribution.

Watts and Strogatz proposed a model for the small-world phenomenon [Watts and Strogatz 1998]. Beginning with a regular lattice of n nodes connected within range k, edges are rewired with probability p. This yields networks with high clustering and short path lengths, interpolating between regular and random structures.

4. Asymptomatic Inference Methods

We assume that the SIS network epidemic process can be observed multiple times. Intuitively, more observations provide more information about the epidemic; however, the time between observations is also an important parameter.

Let $\{t_s\}_{s\in\mathbb{N}}$ denote the observation (snapshot) times of the epidemic process. For a given snapshot i, define the set of nodes observed as infected up to that time as

$$\bigcup_{s=1}^{i} O(t_s),$$

where $O(t_s)$ denotes the set of observed infections at time t_s, as given by Eq. 1. Thus, the set of nodes that can be asymptomatic is given by

$$C(i) = V \setminus \bigcup_{s=1}^{i} O(t_s),$$

as these are the nodes that have yet to be observed as infected. Note that, as i increases, the set $C(i)$ converges to A, the set of asymptomatic nodes.

We consider three inference methods for identifying asymptomatic individuals:

1. **Naïve method:** This approach assumes that all nodes in $C(i)$ are asymptomatic, without further discrimination. Note that the precision of this method increases with the number of snapshots and converges to 1 when $C(i) = A$.
2. **Contact-based method:** For each candidate node $v \in C(i)$, we compute a score reflecting the fraction of its neighbours that have been observed as infected:

   $$c(v,i) = \frac{|N(v) \cap \bigcup_{s=1}^{i} O(t_s)|}{|N(v)|},$$

   where $N(v)$ denotes the set of neighbours of v. A higher score indicates that a candidate node has had greater exposure to infection, suggesting that it may be asymptomatic if it has not itself been observed as infected.
3. **Observed betweenness method [Pinto and Figueiredo 2024]:** This approach measures the centrality of nodes with respect to the observed infection paths. For a given snapshot s, the observed betweenness score of node $v \in C(s)$ is defined as

   $$b(v,s) = \sum_{x,y\in O(t_s)} \frac{\sigma(x,y \mid v)}{\sigma(x,y)},$$

   where $\sigma(x,y)$ denotes the total number of shortest paths between nodes x and y, and $\sigma(x,y \mid v)$ denotes the number of those paths that pass through v. Note that $O(t_s)$ is the set of observed nodes at the single observation time t_s. Nodes with higher observed betweenness are considered more likely to be asymptomatic, as they lie on a larger number of shortest paths connecting observed infections.
   To incorporate temporal information across multiple snapshots, we aggregate these scores over time. Specifically, we define the cumulative observed betweenness (COB) up to snapshot i as

   $$\overline{b}(v,i) = \sum_{s=1}^{i} b(v,s).$$

This aggregated measure is used in all subsequent numerical evaluations. Note that its computational cost is given by $\sum_{s=1}^{i} \mathcal{O}\left(|O(t_s)||E|\right) = \mathcal{O}(i|V||E|)$ where i is the number of snapshots.

These methods provide complementary perspectives: the naïve method establishes a baseline, the contact-based method exploits local exposure information, and the observed betweenness method leverages the global network structure to identify hidden spreaders.

To evaluate the performance of these methods objectively, we employ precision, recall, and the F1 score. For the contact-based and COB methods, nodes are ranked according to their respective scores, and the top-k candidates are considered to be asymptomatic. Intuitively, precision measures the proportion of correctly identified asymptomatic nodes among the top-k, while recall quantifies the proportion of all asymptomatic nodes that are successfully retrieved within the top-k. The F1 score combines these two metrics into a single measure by taking their harmonic mean.

Two remarks are in order. First, the naïve method classifies all candidates as asymptomatic; since $A \subseteq C(t)$ for all t, its recall is always equal to 1, which in turn inflates its F1 score disproportionately. Second, in an epidemic context, screenings are a limited resource (see Section 1), making precision the most relevant performance metric. High precision ensures that the methods effectively identify individuals who should be prioritised for screening. By contrast, recall is inherently constrained by the number of individuals classified as asymptomatic, which is k. Thus, the maximum recall achievable by such methods is $k/|A|$. Therefore, although we report F1 scores in the following section, the discussion primarily focuses on precision.

5. Numerical evaluation

To evaluate the inference methods introduced in Section 4, we designed a suite of experiments covering a range of epidemic dynamics and network structures.[1]

Networks were generated according to three canonical random graph models: Erdős–Rényi (ER), Watts–Strogatz (WS), and Barabási–Albert (BA), presented in Section 3. Their respective parameters were set as follows:

- ER: $p = \frac{8}{3000}$;
- WS: $k = 8$ and $p = 0.3$;
- BA: $m = 4$.

All networks consist of 3000 nodes. These parameter choices ensure that the resulting graphs have approximately the same mean degree across models.

The epidemic parameters were fixed at $\beta = \gamma = 0.01$. Asymptomatic individuals were selected uniformly at random from the node set, according to a prescribed proportion $\rho \in \{0.02, 0.1\}$. Each simulation was initialised with 50 infected individuals and evolved for a burn-in period of 1000 time steps, allowing the dynamics to reach a quasi-stationary regime before any observations were made.

After the burn-in period, 10 snapshots of the epidemic process were recorded. The interval between consecutive snapshots was varied over the set $\{2, 4, 8, 32, 128\}$ in order

[1]The code used to implement the model and run the simulations presented in this paper is publicly available at: github.com/catarcione/sis-asymptomatic.

to assess the impact of observation frequency on the inference task. The performance of the proposed methods is then analysed as a function of the number of available snapshots, following an incremental approach: starting from a single snapshot and progressively incorporating additional observations up to the full set of 10.

As described in Section 4, for the contact-based and COB methods, nodes are ranked according to their respective scores, and performance is evaluated over the top-k candidates. Here, k is defined as a fraction of $|A|$, where A denotes the set of true asymptomatic nodes. In particular, when $k = 1$, the number of selected candidates equals $|A|$; in this case, a perfect method would achieve both precision and recall equal to 1. In what follows the values for $k \in \{0.1, 0.5, 1\}$ are considered.

To ensure statistical robustness, we conducted 100 independent simulations for each combination of network model, asymptomatic proportion, and inter-snapshot interval. Each simulation comprised a newly generated network instance and an independent epidemic realisation. Results are reported as the mean and standard deviation across these realisations.

Figure 2 presents the precision, recall, and F1 score for all three methods as a function of the number of snapshots for two network models. As expected, the performance of all methods improves as the number of snapshots increases. Interestingly, for the COB and Contact methods, precision improves as the top-k threshold decreases (with top-0.1 yielding the best performance), whereas recall deteriorates under the same condition. In contrast, the naïve method always achieves recall 1, but with substantially lower precision than COB in both network models. As a result, its higher F1 scores are mainly driven by this maximal recall. Having established this limitation, we now focus our analysis on precision.

Figure 3 shows the precision of all three methods on the BA network as a function of the number of snapshots. Each subplot corresponds to a different interval between snapshots (2, 4, 32 and 128 time steps). These selected intervals span values both below and above the expected recovery time of an infected individual, given by $\frac{1}{\gamma} = 100$. First, COB consistently achieves substantially higher precision for top-0.1 across all scenarios. More importantly, the interval between snapshots (i.e., the observation frequency) has a pronounced effect on performance. When snapshots are taken at short intervals (e.g., 2 or 4 time steps), each additional snapshot yields only a modest, approximately linear improvement in precision. In contrast, when the interval is large (e.g., 32 or 128 time steps), each additional snapshot leads to a much more significant, near-exponential improvement. Notably, for COB with top-0.1, as few as three snapshots with an interval of 32 time steps are sufficient to achieve perfect precision.

This behaviour is consistent across all methods and can be explained by the decreasing correlation between observations as the interval increases. Less correlated snapshots provide more independent information (e.g., distinct sets of infected and symptomatic individuals), thereby improving the precision of the inference. For example, with COB at top-0.1, two snapshots with an interval of 32 yield a precision exceeding 0.9, whereas an interval of 2 requires six snapshots to surpass the same threshold.

Figure 4 shows precision as a function of the number of snapshots for two different asymptomatic rates (0.02 and 0.1), for ER networks with an inter-snapshot interval of

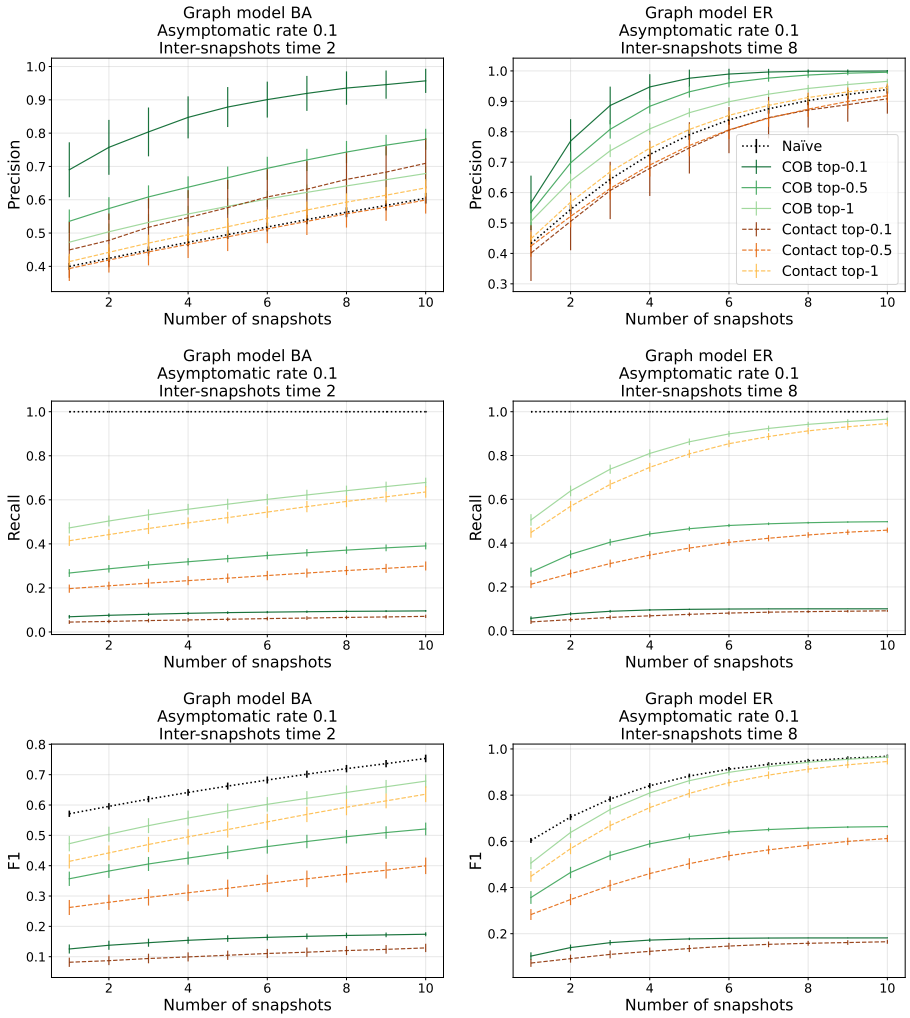

Figure 2. Precision, recall, and F1 score of the naïve, COB, and Contact methods as a function of the number of snapshots for BA and ER network models. Results are shown for different top-k thresholds. Legends are identical across all subplots and are omitted to avoid cluttering the figures.

4 and WS networks with an interval of 8. Intuitively, as the asymptomatic rate increases, asymptomatic nodes constitute a larger proportion of the candidate set, making them easier to identify. Consequently, higher asymptomatic rates lead to improved precision across all methods. For instance, when the asymptomatic rate is 0.1, COB with top-0.1 achieves a precision of approximately 0.9 with five snapshots in both network models. However, when the asymptomatic rate decreases to 0.02 under the same conditions, precision drops significantly, remaining below 0.8 for the WS model and reaching only around 0.6 for the ER model.

5.1. Impact of asymptomatic node selection strategy

To evaluate the effect of asymptomatic node selection, we compare two scenarios: random selection and targeted selection. In the targeted scenario, nodes are ranked according to degree centrality, and the top 10% highest-degree nodes are designated as asymptomatic.

Figure 5 compares the precision obtained under the high-degree selection strategy

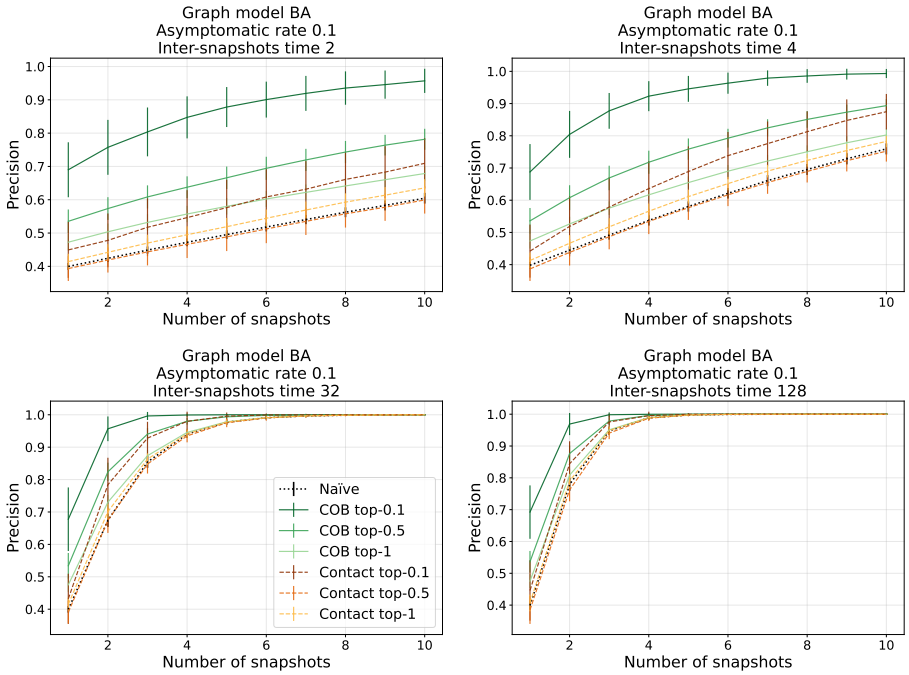

Figure 3. Precision of the naïve, COB, and Contact methods on BA networks as a function of the number of snapshots, for different inter-snapshot intervals (2, 4, 32 and 128 time steps) with an asymptomatic rate of 0.1. Legends are identical across all subplots and are omitted to avoid cluttering the figures.

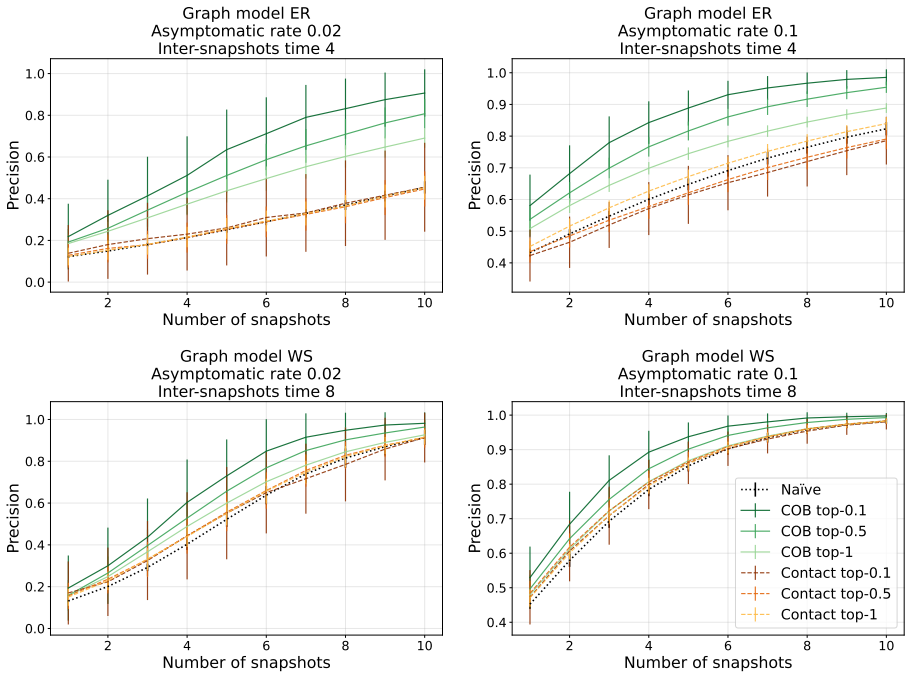

Figure 4. Precision of the naïve, COB, and Contact methods as a function of the number of snapshots, for different asymptomatic rates in ER networks (inter-snapshot interval of 4) and WS networks (interval of 8). Legends are identical across all subplots and are omitted to avoid cluttering the figures.

with the results previously obtained for random asymptomatic node selection. In both network models, COB achieves perfect or near-perfect precision even when only a single snapshot is available. In contrast, the Contact method exhibits lower precision under high-degree selection than in the random selection case, with a relatively small decrease in WS networks but a much stronger degradation in BA networks.

These results can be explained by the different mechanisms underlying each method. Since hub nodes participate in a large number of shortest paths, they naturally receive high COB rankings, which preserves the performance of the COB method even when asymptomatic nodes are concentrated among the highest-degree nodes. The Contact method, however, is more sensitive to this selection strategy. Because this method is normalised by the number of neighbours a node has, the contribution of each infected neighbour is more dampened for high-degree nodes, weakening the signal used by the Contact method and reducing its precision in targeted selection.

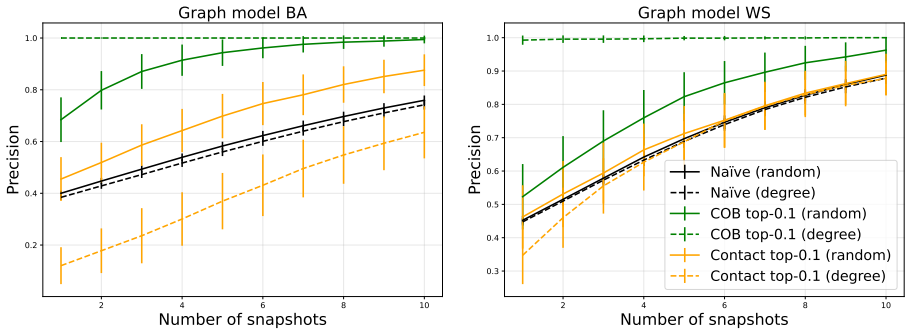

Figure 5. Precision of the naïve, COB, and Contact methods as a function of the number of snapshots for BA (left) and WS (right) networks, with an inter-snapshot interval of 4 and an asymptomatic rate of 0.01. Solid curves correspond to the random selection strategy, whereas dashed curves correspond to the highest-degree selection strategy. The legends are identical across all subplots and are omitted for clarity.

6. Conclusion

This study addressed the problem of identifying asymptomatic nodes in an SIS network epidemic using multiple observations of infected and symptomatic nodes. The proposed method, cumulative observed betweenness (COB), considers the set of candidate nodes at each snapshot, ranks them according to the observed betweenness in that observation, and aggregates this score across snapshots. The top-k nodes in the aggregated ranking that have not been observed as infected in prior observations are then classified as asymptomatic.

An extensive evaluation was performed using different network models and epidemic settings. In terms of precision, COB consistently outperforms the two other approaches across the range of scenarios, indicating its effectiveness as a tool for guiding the allocation of limited screening resources. The results also show that the time interval between snapshots is a fundamental parameter, as the correlation between snapshots decays as this interval increases. Thus, a smaller number of snapshots taken at wider intervals provides significantly more information than many snapshots collected in close succession. This trade-off is particularly relevant because the computational cost of COB

scales directly with the number of snapshots, and can be further investigated in future work.

References

Albert, R. and Barabási, A.-L. (2002). Statistical mechanics of complex networks. *Rev. Mod. Phys.*, 74:47–97.

Arons, M. M., Hatfield, K. M., Reddy, S. C., et al. (2020). Presymptomatic sars-cov-2 infections and transmission in a skilled nursing facility. *New England Journal of Medicine*, 382(22):2081–2090.

Bacaër, N. (2011). *McKendrick and Kermack on epidemic modelling (1926–1927)*, pages 89–96. Springer London, London.

Catarcione Pinto, C., Camacho Novaes de Oliveira, A., Sapienza Luna, R., and Ratton Figueiredo, D. (2026). Identifying asymptomatic nodes in network epidemics using graph neural networks. In *Intelligent Systems*, pages 34–48. Springer Nature Switzerland.

Chen, Y., He, H., Liu, D., et al. (2023). Prediction of asymptomatic covid-19 infections based on complex network. *Optimal Control Applications and Methods*, 44(3):1602–1616.

Huang, S., Sun, J., Feng, L., et al. (2023). Identify hidden spreaders of pandemic over contact tracing networks. *Scientific Reports*, 13(1):11621.

Inui, S., Fujikawa, A., Jitsu, M., et al. (2020). Chest ct findings in cases from the cruise ship diamond princess with coronavirus disease (covid-19). *Radiology: Cardiothoracic Imaging*, 2(2):e200110.

Keeling, M. J. and Eames, K. T. (2005). Networks and epidemic models. *Journal of The Royal Society Interface*, 2(4):295–307.

López Seguí, F., Estrada Cuxart, O., Mitjà i Villar, O., et al. (2021). A cost-benefit analysis of the covid-19 asymptomatic mass testing strategy in the north metropolitan area of barcelona. *International Journal of Environmental Research and Public Health*, 18(13).

Pinto, C. and Figueiredo, D. (2024). Identifying asymptomatic nodes in network epidemics using betweenness centrality. In *Anais do XXIII Workshop em Desempenho de Sistemas Computacionais e de Comunicação*, pages 25–36. SBC.

Quammen, D. (2012). *Spillover: animal infections and the next human pandemic*. WW Norton & Company.

Watts, D. J. and Strogatz, S. H. (1998). Collective dynamics of 'small-world' networks. *Nature*, 393(6684):440–442.

Zhang, R., Tai, J., and Pei, S. (2023). Ensemble inference of unobserved infections in networks using partial observations. *PLOS Computational Biology*, 19(8):1–18.